

Batisivite, the first silicate related to the derbylite-hemloite group

THOMAS ARMBRUSTER^{1,*}, MILEN KADIYSKI¹, LEONID Z. REZNITSKY²,
EVGENY V. SKLYAROV² and EVGENY V. GALUSKIN³

¹ Mineralogical Crystallography, Institute of Geological Sciences, University of Bern, Freiestr. 3, 3012 Bern, Switzerland

*Corresponding author, e-mail: thomas.armbruster@krist.unibe.ch

² Institute of the Earth's Crust (IZK), Siberian Branch, Russian Academy of Sciences, Lermontova Str., 128,
664033 Irkutsk-33, Russia

³ Faculty of Earth Sciences, Department of Geochemistry, Mineralogy and Petrography, University of Silesia,
Będzińska 60, 41-200 Sosnowiec, Poland

Abstract: The crystal structure (space group $P\bar{1}$, $a = 7.5208(4)$, $b = 7.6430(4)$, $c = 9.5724(4)$ Å, $\alpha = 110.204(3)$, $\beta = 103.338(6)$, $\gamma = 98.281(7)^\circ$, $V = 487.14(7)$ Å³, $Z = 1$) of the new mineral batisivite, $(V, Cr)_8Ti_6[Ba(Si_2O_7)]O_{22}$, has been determined and refined from single-crystal X-ray data to $R = 2.59\%$. Strong and sharp X-ray reflections define a C-centred monoclinic lattice with $a = 4.9878(3)$, $b = 14.1899(16)$, $c = 7.0813(2)$ Å, $\beta = 103.598(4)^\circ$, characteristic for members of the derbylite group. Considering additional weak and slightly diffuse reflections, the pattern could be indexed with a primitive triclinic cell as cited above. There are eight metal (M) sites, with M1–M4 defining octahedral α -PbO₂ double chains and M5–M8 defining octahedral columns as in the structure of V₃O₅. The stacking of both units defines the structure of the derbylite type with channels that may be described as chains of empty cube-octahedra running parallel to [011] in triclinic setting. In batisivite adjacent cube-octahedra are alternately occupied by Ba and disilicate units, lowering the symmetry to triclinic. However, Ba-disilicate order is not complete. One cube-octahedron is statistically filled by *ca.* $\frac{3}{4}$ Ba and $\frac{1}{4}$ disilicate, the other is occupied by *ca.* $\frac{3}{4}$ disilicate and $\frac{1}{4}$ Ba. This type of disorder is in qualitative agreement with the observed slight diffusivity of the super-structure reflections. The bridging oxygen of the disilicate group occupies the same site as disordered central Ba.

Key-words: batisivite, disilicate, derbylite-hemloite group of minerals, single crystal X-ray diffraction, structure solution.

Introduction

Batisivite, with empirical formula $(V_{4.77}^{3+}V_{0.75}^{4+}Cr_{2.20}Fe_{0.25}Nb_{0.03})_{\Sigma 8.0}(Ti_{5.41}V_{0.59}^{4+})_{\Sigma 6.0}[Ba_{1.01}Mg_{0.02}(Si_{1.40}Al_{0.48})O_{6.58}]O_{22.38}$, ideal $(V, Cr)_8Ti_6[Ba(Si_2O_7)]O_{22}$ has been recently described as a new mineral (Reznitsky *et al.*, 2007), which occurs as an accessory mineral in quartz layers from the metamorphosed Cr-V-bearing carbonate-siliceous sediments of the Sludyanka complex, Southern Lake Baikal, Siberia, Russia. The Pereval marble quarry is the type locality for natalyite, florensovite, kalininite, magnesiocoulsonite, chromphyllite and vanadiumdravite. Associated minerals are: quartz, Cr-V-bearing diopside and tremolite, calcite, schreyerite, berdesinskiite, ankangite, V-bearing titanite, eskolaite-karelianite, chromite-coulsonite, Cr-bearing goldmanite, dravite-vanadiumdravite, uraninite, chernykhite-roscoelite, albite, barite, zircon, and unnamed oxides of V, Cr, Ti, U (Reznitsky & Sklyarov, 1996; Konev *et al.*, 2001). Frequently batisivite forms intergrowths with schreyerite $V_2Ti_3O_9$ (Reznitsky *et al.*, 2007). Batisivite occurs as anhedral grains with black color and streak, with a size up to 0.15–0.20 mm. The name is for its chemical composition with barium, titanium,

silicon, and vanadium as the most important cationic components. This paper describes the crystal structure of this unusual derbylite-group mineral.

Experimental methods

Batisivite was concentrated by magnetic and heavy liquid separation. Few grains were selected for structural investigation by energy dispersive analyses using a Philips XL30 scanning electron-microscope.

Composition of batisivite was investigated by means of a CAMECA SX-100 electron-microprobe at 15 kV and 20 nA, beam size 1–2 µm. Standards, characteristic lines, and analytical crystals are given below and were selected accounting for difficulties of the mineral composition containing simultaneously Ti, V, Cr, and Ba: LiNbO₃ and metallic Nb–NbLα (PET); diopside – MgKα, SiKα (TAP); orthoclase–AlKα (TAP), rutile–TiKα (LIF), barite–BaLβ (PET), Cr₂O₃–CrKβ (PET), Fe₂O₃–FeKα (LIF), metallic V–VKα (LIF).

X-ray diffraction intensity-data were collected with an Enraf-Nonius CAD4 diffractometer using graphite

Table 1. Chemical composition (mean of eight point analyses) of the batisvite grain used for single-crystal X-ray structure analysis; data from microprobe analyses. Formula normalized on V + Cr + Ti + Fe + Nb = 14.

	mean $\Sigma 8$	s.d.	apfu	
V ₂ O ₃	32.44	1.10	5.868	} 8.025
Cr ₂ O ₃	12.09	0.98	2.157	
TiO ₂	33.51	0.61	5.687	
Fe ₂ O ₃	1.51	0.06	0.256	
Nb ₂ O ₅	0.30	0.08	0.032	} 5.975
SiO ₂	6.20	0.14	1.399	
Al ₂ O ₃	1.91	0.09	0.508	
BaO	11.78	0.18	1.042	} 1.907
MgO	0.06	0.01	0.020	
Total	99.80			} 1.062

Table 2. Details of X-ray data collection of batisvite.

space group	$P\bar{1}$ (No. 2)
a, b, c (Å)	7.5208(4), 7.6430(4), 9.5724(4)
α, β, γ (°)	110.204(3), 103.338(6), 98.281(7)
V (Å ³)	487.14(7)
diffractometer	Enraf Nonius CAD4
X-ray radiation	MoK α
X-ray power	50 kV, 40 mA
temperature	293 K
crystal size	75 × 125 × 150 μm^3
upper θ limit	30°
h, k, l limit	-10 ≤ h ≤ 10, -10 ≤ k ≤ 10, -1 ≤ l ≤ 13
reflections measured	2605
unique reflections	2222
reflections > 4 σ (F)	1822
absorption correction	empirical ψ -scans
R (int) %	1.04
R (σ) %	2.02
Number of least square parameters	215
GooF	1.067
$R1\%$, $F_o > 4\sigma(F_o)$	2.59
$R1\%$, all data	3.83
wR % (on F^2)	7.16

monochromated MoK α -X-radiation. Data reduction, including background and Lorentz polarization correction, was carried out with the SDP program system (Enraf Nonius, 1983). An empirical absorption correction using the ψ -scan technique was applied. Experimental details of data collection and structure refinement are summarized in Table 2.

The diffraction pattern is characterized by strong, sharp reflections, defining a C -centred monoclinic lattice with $a = 4.9878(3)$, $b = 14.1899(16)$, $c = 7.0813(2)$ Å, $\beta = 103.598(4)^\circ$. These cell dimensions are characteristic for members of the derbylite group. However, there are additional weak reflections revealing a half-width about 30% greater (slightly diffuse) than the sharp reflections consis-

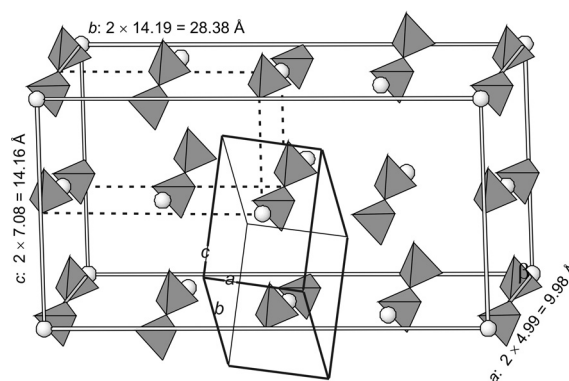


Fig. 1. Ordered arrangement of Si₂O₇ and Ba in batisvite; the octahedral framework is omitted and only the dominant Ba and Si₂O₇ sites are shown. Dashed lines indicate the C -centred monoclinic subcell, which is in batisvite only obeyed for the octahedral framework but not for the distribution of the occupants within the cubo-octahedral cages. The largest cell represents a pseudo-monoclinic supercell with the same orientation as the basic C -centred subcell but all axes are doubled. The supercell is A , B , and C -centred and displays an awkward representation of Ba and Si₂O₇ order. The small cell with solid thin lines depicts the triclinic cell, which is sufficient for the description of Ba and Si₂O₇ order.

tent with the monoclinic subcell. In reciprocal space these additional reflections are shifted $1/2, 1/2, 1/2$ relative to the reflections of the monoclinic subcell. Considering all reflections, the pattern can be indexed with a primitive triclinic unit-cell given in Table 2. The Niggli-reduced triclinic cell can be transformed by the matrix (0 1 1, 4 1 1, 0 1 -1) to a cell with the same orientation as the C -centred monoclinic subcell (Fig. 1). However, this pseudo-monoclinic “supercell” has all axes doubled ($V = 3897$ Å³). Thus the volume is eight-times that of the triclinic cell. Triclinic cell dimensions were refined from the angular settings of 25 reflections ($23^\circ < \theta < 29^\circ$) where each reflection was centred for four diffracting positions (positive and negative θ) to reduce systematic errors.

Structure solution was performed by direct methods using the program SHELXS and subsequent refinement was done with the program SHELXL (Bruker, 1997) applying neutral atom scattering factors. Because Ti, V, Cr have similar scattering factors and cannot be distinguished by this type of routine X-ray analysis, V scattering factors were used to model mixtures of transition elements on M sites. M1–M4 define octahedral sites commonly described as α -PbO₂ double chains and M5–M8 define octahedral sites forming columns as in the structure of V₃O₅. Partial occupancy was considered for Ba and Si.

Results

Atomic coordinates and anisotropic displacement parameters are given in Tables 3 and 4. Selected bond lengths are summarized in Table 5. Stacking of α -PbO₂ double chains and columns as in the structure of V₃O₅ (Fig. 2) forming interstitial channels define the structure of the derbylite

Table 3. Atomic positional parameters and B_{eq} values for batisivite.

atom	occupancy	x	y	z	B_{eq} (\AA^2)
Ba1	0.772(2)	1/2	0	1/2	0.692(7)
Ba2	0.248(2)	1/2	-1/2	0	0.99(2)
Si1	0.751(2)	0.5002(2)	-0.4057(2)	0.1821(1)	0.31(2)*
Si2	0.227(2)	0.5009(6)	-0.0941(6)	0.3180(5)	0.31(2)*
OD1	0.227(2)	1/2	0	1/2	0.692(7)
OD2	0.751(2)	1/2	-1/2	0	0.99(2)
M1		0.11201(8)	0.18952(8)	0.50638(6)	0.372(9)
M2		0.88625(8)	0.38522(8)	0.69966(7)	0.402(9)
M3		0.88360(8)	-0.12456(9)	0.19818(7)	0.434(9)
M4		0.11820(8)	0.68600(8)	0.00635(7)	0.465(8)
M5		0.26870(9)	-0.30331(9)	0.69272(7)	0.79(1)
M6		0.73514(9)	-0.18684(9)	0.80932(7)	0.733(9)
M7		1/2	-1/2	1/2	0.36(1)
M8		1/2	0	0	0.62(1)
O1		0.1001(3)	-0.1468(3)	0.6757(3)	0.48(3)
O2		0.4996(3)	-0.5644(4)	0.2762(3)	0.76(4)
O3		0.9315(3)	0.6065(3)	0.1083(3)	0.38(3)
O4		0.9050(3)	-0.3443(3)	0.8271(3)	0.56(4)
O5		0.9252(3)	0.1077(3)	0.6062(3)	0.40(3)
O6		0.6915(4)	-0.2145(4)	0.2943(3)	0.99(5)
O7		0.5001(3)	-0.0759(4)	0.7824(3)	0.71(4)
O8		0.0959(3)	-0.5463(3)	0.6230(3)	0.59(3)
O9		0.9010(3)	0.0535(3)	0.8744(3)	0.49(3)
O10		0.3031(3)	0.2567(3)	0.4147(3)	0.47(3)
O11		0.3103(4)	-0.3093(4)	0.1989(3)	0.89(5)
O12		0.3019(3)	0.7595(3)	0.9160(3)	0.48(3)
O13		0.7002(3)	-0.1406(3)	0.0153(3)	0.43(3)
O14		0.6947(3)	0.3540(3)	0.5128(3)	0.44(3)

* Starred atoms were refined isotropically.

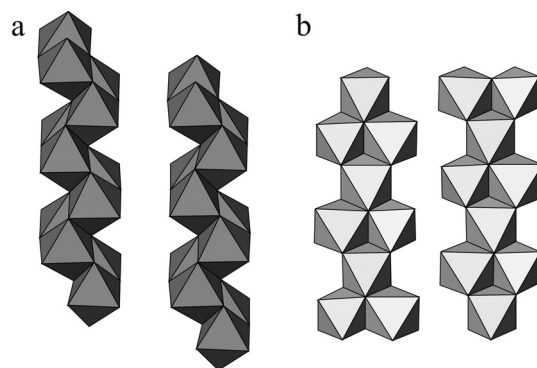


Fig. 2. (a) $\alpha\text{-PbO}_2$ -type zigzag double chains of edge-sharing MO_6 octahedra and (b) V_3O_5 -type columns of edge-sharing MO_6 octahedra. M—Ti, Fe, or V.

type (*e.g.*, Berlepsch & Armbruster, 1998). The channels may be described by chains of empty cube-octahedra running parallel to [011] in triclinic setting (Fig. 3a). Adjacent cube-octahedra are alternately occupied by Ba and disilicate units (Fig. 1 and 4). This order pattern is responsible for the triclinic symmetry. However, Ba-disilicate order is not complete. One cube-octahedron is statistically filled by *ca.* $3/4$ Ba and $1/4$ disilicate, the other is occupied by *ca.* $3/4$ disilicate and $1/4$ Ba. This type of disorder is in qualitative agreement with the observed slight diffusivity of the super-

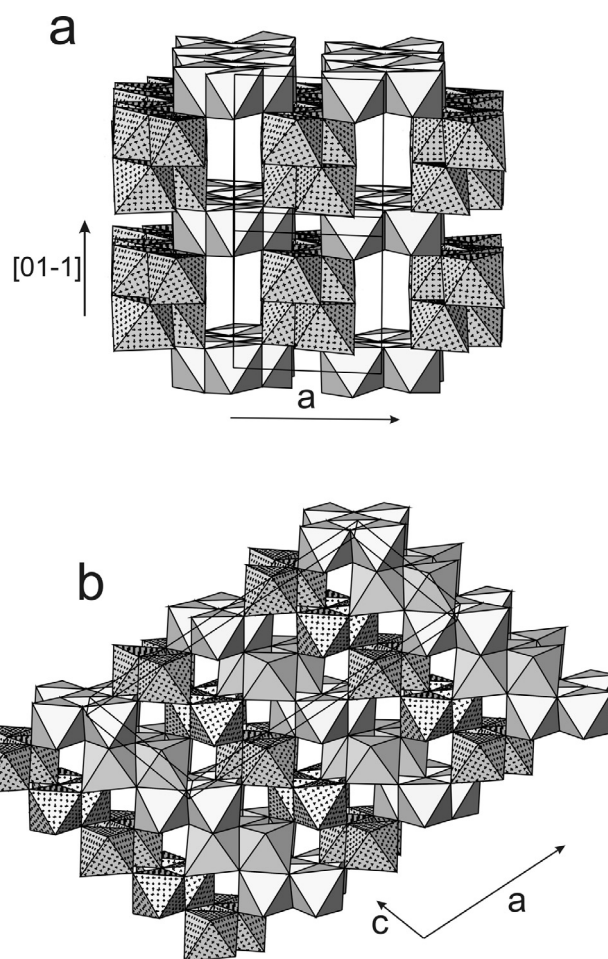


Fig. 3. (a) Construction scheme of the octahedral framework of derbylite-hemloite group minerals assembled of $\alpha\text{-PbO}_2$ -type zigzag double-chains (cross-hatched) and V_3O_5 -type columns of edge-sharing MO_6 octahedra (white). Unit cell directions conform to the triclinic cell of batisivite. (b) Polyhedral model of schreyerite (Döbelin *et al.*, 2006) projected parallel to the b -axis. The structure is interpreted as a 1:1 polysome composed of berdesinskiite-type (V_3O_5 -type) chains (white octahedra) and $\alpha\text{-PbO}_2$ -type chains (cross-hatched octahedra).

structure reflections. The bridging oxygen of the disilicate group occupies the same site as disordered central Ba. For this reason displacement parameters of Ba and bridging oxygen (OD) were constrained to be equal. Furthermore, occupancies for OD and connected Si were set equal. To reduce possible correlations between Si occupancy and Si displacement parameters, Si1 and Si2 were refined isotropically and constrained to a common value.

The refined composition of the studied crystal is $(\text{Ti}, \text{Cr}, \text{V})_{14}\text{Ba}_{1.02}[\text{Si}_2\text{O}_7]_{0.98}\text{O}_{22.12}$, which agrees nicely with the analytically determined composition of $(\text{V}_{4.955}^{3+}\text{V}_{0.600}^{4+}\text{Cr}_{2.157}\text{Fe}_{0.256}\text{Nb}_{0.032})_{\Sigma 8.0}(\text{Ti}_{5.687}\text{V}_{0.313}^{4+})_{\Sigma 6.0}[\text{Ba}_{1.042}\text{Mg}_{0.020}(\text{Si}_{1.467}\text{Al}_{0.533}\text{O}_7)_{0.953}]\text{O}_{22.283}$ (Table 1) and with empirical formula $(\text{V}_{4.77}^{3+}\text{V}_{0.75}^{4+}\text{Cr}_{2.20}\text{Fe}_{0.25}\text{Nb}_{0.03})_{\Sigma 8.0}(\text{Ti}_{5.41}\text{V}_{0.59}^{4+})_{\Sigma 6.0}[\text{Ba}_{1.01}\text{Mg}_{0.02}(\text{Si}_{1.49}\text{Al}_{0.51}\text{O}_7)_{0.94}]\text{O}_{22.38}$, calculated on the basis of 237 analyses (Reznitsky *et al.*, 2007).

Table 4. Anisotropic displacement parameters for batisivite.

atom	U_{11}	U_{22}	U_{33}	U_{12}	U_{13}	U_{23}
Ba1	0.0060(2)	0.0056(2)	0.0125(2)	0.0006(1)	0.0021(2)	0.0018(1)
Ba2	0.0137(5)	0.0072(5)	0.0174(6)	0.0048(4)	0.0031(4)	0.0060(4)
OD1	0.0060(2)	0.0056(2)	0.0125(2)	0.0006(1)	0.0021(2)	0.0018(1)
OD2	0.0137(5)	0.0072(5)	0.0174(6)	0.0048(4)	0.0031(4)	0.0060(4)
M1	0.0040(3)	0.0056(3)	0.0036(3)	-0.0001(2)	0.0011(2)	0.0012(2)
M2	0.0047(3)	0.0064(3)	0.0041(3)	0.0019(2)	0.0010(2)	0.0020(2)
M3	0.0049(3)	0.0068(3)	0.0051(3)	0.0019(2)	0.0017(2)	0.0023(2)
M4	0.0055(3)	0.0062(3)	0.0050(3)	0.0001(2)	0.0017(2)	0.0015(2)
M5	0.0130(3)	0.0105(3)	0.0069(3)	0.0026(3)	0.0035(2)	0.0035(2)
M6	0.0112(3)	0.0095(3)	0.0074(3)	0.0023(2)	0.0036(2)	0.0032(2)
M7	0.0042(3)	0.0046(3)	0.0037(3)	0.0006(3)	0.0012(3)	0.0006(3)
M8	0.0070(4)	0.0085(4)	0.0068(4)	0.0010(3)	0.0024(3)	0.0017(3)
O1	0.006(1)	0.007(1)	0.005(1)	0.0045(9)	0.000(1)	0.0018(9)
O2	0.006(1)	0.010(1)	0.009(1)	0.002(1)	0.001(1)	0.000(1)
O3	0.006(1)	0.004(1)	0.004(1)	0.0015(9)	0.0013(9)	0.0016(9)
O4	0.006(1)	0.008(1)	0.007(1)	0.0031(9)	0.001(1)	0.002(1)
O5	0.005(1)	0.005(1)	0.005(1)	0.0002(9)	0.0012(9)	0.0023(9)
O6	0.006(1)	0.023(1)	0.010(1)	0.002(1)	0.002(1)	0.010(1)
O7	0.007(1)	0.011(1)	0.006(1)	0.001(1)	0.002(1)	0.000(1)
O8	0.007(1)	0.006(1)	0.008(1)	-0.0009(9)	0.004(1)	0.0014(9)
O9	0.006(1)	0.005(1)	0.008(1)	-0.0006(9)	0.003(1)	0.0022(9)
O10	0.005(1)	0.006(1)	0.006(1)	-0.0010(9)	0.0019(9)	0.0030(9)
O11	0.006(1)	0.021(1)	0.009(1)	0.002(1)	0.002(1)	0.009(1)
O12	0.006(1)	0.006(1)	0.006(1)	-0.0005(9)	0.003(1)	0.0019(9)
O13	0.006(1)	0.007(1)	0.004(1)	0.0036(9)	0.0009(9)	0.0029(9)
O14	0.005(1)	0.006(1)	0.006(1)	0.0028(9)	0.0010(9)	0.0035(9)

Table 5. Selected bond distances (Å) for batisivite.

Ba1	O14	2 × 2.833(2)	M1	O10	1.944(2)	O11	2.048(3)		
	O10	2 × 2.845(3)		O1	1.965(3)		O3	2.054(2)	
	O11	2 × 2.891(3)		O8	1.979(3)		Mean	1.997	
	O5	2 × 3.017(3)		O5	2.014(2)		M5	O1	1.882(3)
	O6	2 × 2.898(3)		O6	2.056(3)		O8	1.906(2)	
	O7	2 × 2.955(3)		O5	2.095(2)		O14	1.962(2)	
Mean	2.907	Mean	2.009	O12	1.967(3)				
Ba2	O11	2 × 2.778(3)	M2	O14	1.936(3)	O7	2.048(2)		
	O6	2 × 2.784(3)		O8	1.964(2)	O2	2.150(3)		
	O2	2 × 2.852(3)		O4	1.969(2)	Mean	1.986		
	O12	2 × 2.864(3)		O3	1.999(3)	M6	O9	1.873(2)	
	O13	2 × 2.875(3)		O11	2.066(2)	O4	1.895(3)		
	O3	2 × 3.061(3)		O5	2.091(2)	O10	1.961(3)		
Mean	2.869	Mean	2.004	O13	1.967(3)				
Si1	OD2	1.640(1)	M3	O13	1.916(3)	O7	2.070(3)		
	O11	1.714(3)		O1	1.976(2)	O2	2.167(2)		
	O6	1.720(3)		O9	1.982(2)	Mean	1.989		
	O2	1.743(3)		O5	2.032(3)	M7	O14	2 × 1.972(3)	
	Mean	1.704		O6	2.042(2)	O10	2 × 1.980(2)		
Si2	OD1	1.642(4)	Mean	O3	2.056(3)	O2	2 × 2.024(3)		
	O11	1.825(4)		2.001	Mean	1.992			
	O6	1.828(5)		M4	O12	1.907(2)	M8	O7	2 × 1.959(3)
	O7	1.864(6)			O9	1.969(3)	O12	2 × 1.970(2)	
Mean	1.790	O4	1.979(3)	O13	2 × 1.978(3)				
			O3	2.022(2)	Mean	1.969			

Table 6. Members of the derbylite-hemloite group (for references see text).

Mineral	Symmetry	Unit cell dimensions		Type locality
Batisivite	Triclinic, $P\bar{1}$	$a = 7.5208(4) \text{ \AA}$ $b = 7.6430(4) \text{ \AA}$ $c = 9.5724(4) \text{ \AA}$ $Z = 1$	$\alpha = 110.204(3)^\circ$ $\beta = 103.338(6)^\circ$ $\gamma = 98.281(1)^\circ$ $V = 487.14(7) \text{ \AA}^3$	Sludyanka, Siberia, Russia
Hemloite	Triclinic, $P\bar{1}$	$a = 7.158(1) \text{ \AA}$ $b = 7.552(1) \text{ \AA}$ $c = 16.014(3) \text{ \AA}$ $Z = 2$	$\alpha = 89.06(1)^\circ$ $\beta = 104.32(2)^\circ$ $\gamma = 84.97(1)^\circ$ $V = 834.8 \text{ \AA}^3$	Hemlo, Ontario, Canada
Barian Tomichite	Monoclinic, $A2/m$	$a = 7.105(4) \text{ \AA}$ $b = 14.217(4) \text{ \AA}$ $c = 5.043(2) \text{ \AA}$ $Z = 2$	$\beta = 104.97(7)^\circ$ $V = 492.1 \text{ \AA}^3$	Hemlo, Ontario, Canada
Tomichite	Monoclinic, $P2_1/m$	$a = 7.119(3) \text{ \AA}$ $b = 14.176(5) \text{ \AA}$ $c = 4.992(2) \text{ \AA}$ $Z = 2$	$\beta = 105.05(1)^\circ$ $V = 486.5 \text{ \AA}^3$	Kalgoorlie, W Australia
Derbylite	Monoclinic, $P2_1/m$	$a = 7.160(1) \text{ \AA}$ $b = 14.347(3) \text{ \AA}$ $c = 4.970(1) \text{ \AA}$ $Z = 2$	$\beta = 104.61(2)^\circ$ $V = 494.0 \text{ \AA}^3$	Tripuhy, Ouro Preto, Brazil
Graeserite	Monoclinic, $C2/m$	$a = 5.0053(4) \text{ \AA}$ $b = 14.272(1) \text{ \AA}$ $c = 7.1736(6) \text{ \AA}$ $Z = 2$	$\beta = 105.165(2)^\circ$ $V = 494.6 \text{ \AA}^3$	Gorb, Binntal, Switzerland

Note: $C2/m$ is the standard setting of space group No. 12. Some authors use the non-standard $A2/m$ setting (a and c axes interchanged) to conform to the axial orientation of space group $P2_1/m$ found for tomichite and derbylite.

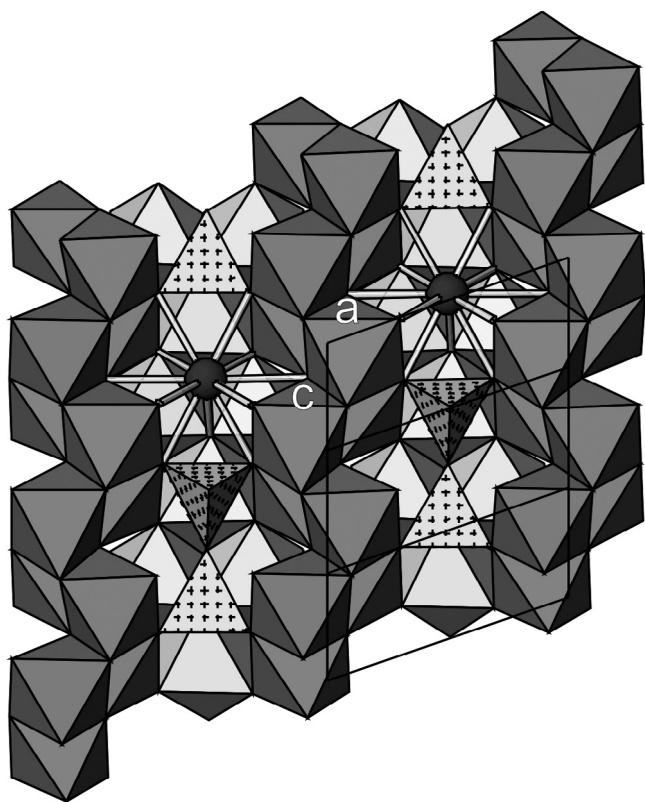


Fig. 4. Polyhedral model of the structure of batisivite with Ba (spheres with bonds) and disilicate units (cross-hatched tetrahedra) alternating in the cube-octahedral cavities. Channels run parallel to [011].

Comparison with the analysed composition indicates that Si is partly replaced by Al. This is also supported by slightly increased Si-O distances. In addition, the partly disordered disilicate-Ba distribution influences the bond lengths. The cube-octahedron with the high Ba occupancy expands the cavity thus the disordered disilicate unit reveals rather unrealistic (Si, Al)-O bond lengths in the range of *ca.* 1.85 Å (Table 5). The correctness of this interpretation is validated by the observed average (Si, Al)-O distances (< 1.75 Å) for the cube-octahedron with low (*ca.* 25%) occupancy of Ba.

Discussion

Batisivite $[(\text{Ti}, \text{V}, \text{Cr})_{14}\text{Ba}[\text{Si}_2\text{O}_7]\text{O}_{22}]$ is homeotypic with the members of the derbylite-hemloite group of minerals, Dana class 46.2.3; Strunz & Nickel (2001) class 4.JB.55 (Table 6). The group consists of derbylite $[\text{Fe}_4\text{Ti}_3\text{SbO}_{13}(\text{OH})]$ (Hussak & Prior, 1897; Moore & Araki, 1976), tomichite $[(\text{V}, \text{Fe})_4\text{Ti}_3\text{AsO}_{13}(\text{OH})]$ (Nickel & Grey, 1979; Grey *et al.*, 1987), barian tomichite $[\text{Ba}_{0.5}(\text{As}_2)_{0.5}\text{Ti}_2(\text{V}, \text{Fe})_5\text{O}_{13}(\text{OH})]$ (Grey *et al.*, 1987), hemloite $[(\text{Ti}, \text{V}, \text{Fe})_{12}(\text{As}, \text{Sb})_2\text{O}_{23}(\text{OH})]$ (Harris *et al.*, 1989) and graeserite $[(\text{Fe}, \text{Ti})_7\text{As}(\text{O}, \text{OH})_{14}]$ (Krzemnicki & Reusser, 1998; Berlepsch & Armbruster, 1998).

Common to all of the above structures are α - PbO_2 -type zigzag double-chains of edge-sharing MO_6 octahedra (Fig. 2a), with M being Ti, Fe or V. These chains are connected to adjacent V_3O_5 -type columns of edge-sharing MO_6 octahedra (Fig. 2b) to form a framework with cube-octahedral cavities (Fig. 4 and 5). In case of derbylite, tomichite, hemloite, and graeserite, those cavities (Fig. 5)

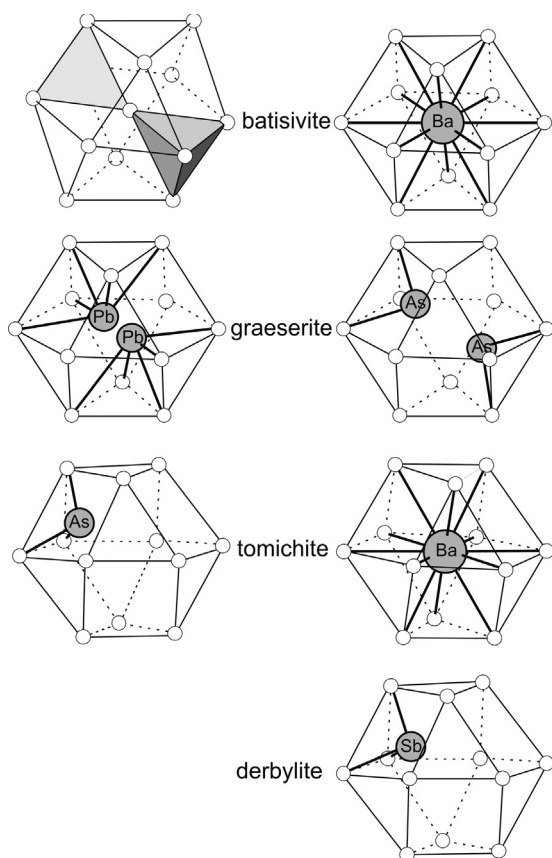


Fig. 5. Coordination of the extraframework cations in the cube-octahedral cavities in the structures of batisivite, graeserite, tomichite and barian tomichite, and derbylite; small white spheres represent oxygen atoms.

accommodate isolated SbO_3 or AsO_3 pyramids; in the ordered structure of barian tomichite, these cavities are occupied by alternating $\text{SbO}_3/\text{AsO}_3$ pyramids and Ba atoms whereas in batisivite these sites are occupied by alternating disilicate units and Ba atoms (Fig. 1 and 4). Diffuse superlattice reflections leading to apparent doubling of the a and c axes have already been reported for barian tomichite (Grey *et al.*, 1987) but the corresponding structure refinement is based on the sharp reflections of the subcell only.

All derbylite-hemloite-group minerals, except batisivite, have a ratio of octahedral cations to oxygen of 1/2 and are hydroxylated. In batisivite, the ratio of octahedral cations to oxygen is 14/29. The one excess oxygen is centred in the cube-octahedra and connects the $(\text{Si, Al})\text{O}_4$ tetrahedra to disilicate groups. To maintain the derbylite-characteristic stoichiometry Reznitsky *et al.* (2007) suggested for batisivite the formula notation $(\text{Ti, V, Cr})_{14}\text{Ba}[\text{Si}_2\text{O}]_{28}$. In this notation, Si_2O acts as a quasi-molecule (Handke & Mozgawa, 1995) occupying the structural voids. If half of the cube-octahedra are filled with disilicate groups, batisivite will not be hydroxylated. The octahedral framework structure exhibits two oxygen sites (O6, O11), which only bond to two octahedra and may be for this reason regarded potential OH sites. However, for the idealized composition $(\text{Ti, V, Cr})_{14}\text{Ba}[\text{Si}_2\text{O}_7]_{22}$, O6 and O11 are addition-

ally bonded to Si and hydroxylation must be excluded for bond-strengths arguments. This is also true if Si is partly substituted by Al. On the other hand, partial hydroxylation may occur if the Ba/disilicate ratio is > 1 . This model is in agreement with the observations by Reznitsky *et al.* (2007) that Raman spectra of batisivite, covering the OH stretching region, do not indicate significant hydroxylation.

In addition, more than 50% disilicate groups occupying the cube-octahedral voids are not possible because this would lead to edge-sharing tetrahedra, short Si-Si separations, and overbonding of O6 and O11 (in that case O6 and O11 were connected to two Si tetrahedra and two (V, Ti, Cr) octahedra). Thus, batisivite with 50% of the cube-octahedral voids occupied by Ba and the other 50% by the “pseudomolecule” Si_2O is a well-defined end-member.

Within the octahedral framework, there are two oxygen sites, which are four-coordinated: O3 (bonded to M2, M3 and $2 \times$ to M4) and O5 (bonded to M2, M3 and $2 \times$ to M1). This arrangement may indicate that M1–M4, assembling the $\alpha\text{-PbO}_2$ -type zigzag chains, are preferentially occupied by three-valent cations, thus reducing overbonding of O3 and O5. Consequently, M5–M8 (V_3O_5 ribbons) are preferentially occupied by M^{4+} . Neither the spreading of M–O distances in individual octahedra nor the average $\langle \text{M–O} \rangle$ distances provide any convincing clue for M^{4+} and M^{3+} preferences. $\langle \text{M–O} \rangle$ distances range from 1.969 to 2.009 Å (Table 5) and all fall into the range given by Schindler *et al.* (2000) for V^{3+} . Although at the edge of significance, average $\langle \text{M–O} \rangle$ distances (Table 5) for M1–M4 ($\alpha\text{-PbO}_2$ -type chain), preferentially occupied by M^{3+} , are slightly longer than 2.0 Å whereas the corresponding distances for M5–M8 (V_3O_5 -like ribbons), preferentially occupied by M^{4+} , are slightly shorter than 2.0 Å. Ionic radii for octahedral coordination (Shannon, 1976) are also in agreement with this assignment. Ti^{4+} (0.605 Å) and V^{4+} (0.58 Å) are slightly smaller than the three-valent transition metals V^{3+} (0.64 Å) and Cr^{3+} (0.615 Å).

Reznitsky *et al.* (2007) demonstrated that batisivite contains both V^{3+} and V^{4+} (up to 2 V^{4+} per formula unit). The amount of V^{4+} , calculated for charge balance, exhibits a negative correlation with (Ti + Si) suggesting that V^{4+} replaces octahedral Ti^{4+} . According to mineral-database screening of oxides (Bartholomew *et al.*, 2005), only zoltaiite $\text{BaV}_2^{4+}\text{V}_{12}^{3+}\text{Si}_2\text{O}_{27}$ and häggite $\text{V}^{4+}\text{V}^{3+}\text{O}_2(\text{OH})_3$ reveal mixed $\text{V}^{3+}\text{–V}^{4+}$ valences. We add to this short list that significant V^{4+} beside dominant V^{3+} is also found in batisivite (Reznitsky *et al.*, 2007), schreyerite and berdesinskiite (Döbelin *et al.*, 2006).

Schreyerite and batisivite not only occur intergrown with each other (Reznitsky *et al.*, 2007) but are also assembled of the same structural modules. Döbelin *et al.* (2006) interpreted schreyerite $\text{V}_2\text{Ti}_3\text{O}_9$ as a 1:1 polysome composed of slabs of berdesinskiite V_2TiO_5 (V_3O_5 structure type) and Ti_2O_4 (a high pressure phase of TiO_2 with $\alpha\text{-PbO}_2$ structure). These slabs (Fig. 3b) are interconnected to staircase-like layers. In batisivite V_3O_5 -like chains extend along [011] and form parallel to (0–11) a layer-like unit with individual chains separated by gaps. The next

layer along [01–1] is formed by α -PbO₂-like double-chains arranged in a staggered fashion relative to the adjacent layers (Fig. 3a). This construction system leads to open channels parallel to [011]. The topological similarity of modules assembling batisivite and schreyerite is contrasted by the distribution of octahedral M³⁺ and M⁴⁺ within the different slabs. Döbelin *et al.* (2006) suggested that in schreyerite M³⁺ concentrates in the V₃O₅-modules yielding the composition V₂TiO₅. Their main arguments were face-sharing octahedra in the V₃O₅-module, which are not favoured by M⁴⁺ for repulsive reasons. The α -PbO₂-like modules in schreyerite are occupied by M⁴⁺ to satisfy V₂Ti₃O₉ stoichiometry. For batisivite we suggested M³⁺ for the α -PbO₂-like double-chains and M⁴⁺ for the V₃O₅-like chains. The difference in the M³⁺, M⁴⁺ distribution between the two structures is due to the different linkage of the modules.

Acknowledgements: The manuscript benefited from the reviews by Marc Cooper and Andrew Locock, which is highly appreciated. T.A. acknowledges support by the Swiss National Science Foundation, grant 200020-112198 “Crystal Chemistry of Minerals” and L.R. acknowledges support by the Russian Foundation for Basic Research, grant 06-05-64300 “Main features of formation of Cr-V-minerals and their parageneses in metamorphic processes”.

References

- Bartholomew, P.R., Mancini, F., Cahill, C., Harlow, G.E., Bernhardt, H.J. (2005): Zoltaiite, a new barium-vanadium nesosubsilicate mineral from British Columbia: Description and crystal structure. *Am. Mineral.*, **90**, 1655-1660.
- Berlepsch, P. & Armbruster, Th. (1998): The crystal structure of Pb²⁺-bearing graeserite, Pb_{0.14}(Fe, Ti)₇AsO_{12+x}(OH)_{2-x}, a mineral of the derbylite group. *Schweiz. Mineral. Petrogr. Mitt.*, **78**, 1-9.
- Bruker (1997): SHELXTL, Version 5.1. Bruker AXS Inc., Madison, Wisconsin, USA.
- Döbelin, N., Reznitsky, L.Z., Sklyarov, E.V., Armbruster, Th., Medenbach, O. (2006): Schreyerite, V₂Ti₃O₉: New occurrence and crystal structure. *Am. Mineral.*, **91**, 196-202.
- Enraf, Nonius (1983): Structure determination package (SDP). Enraf Nonius, Delft, the Netherlands.
- Grey, I.E., Madsen, I.C., Harris, D.C. (1987): Barian tomichite, Ba_{0.5}(As₂)_{0.5}Ti₂(V,Fe)₅O₁₃(OH), its crystal structure and relationship to derbylite and tomichite. *Am. Mineral.*, **72**, 201-208.
- Handke, M. & Mozgawa, W. (1995): Model quasi-molecule Si₂O as an approach in the IR spectra description glassy and crystalline framework silicates. *J. Mol. Str.*, **348**, 341-344.
- Harris, D.C., Hoskins, B.F., Grey, I.E., Criddle, A.J., Stanley, C.J. (1989): Hemloite (As,Sb)₂(Ti, V, Fe, Al)₁₂O₂₃(OH): A new mineral from the Hemlo gold deposit, Hemlo, Ontario, and its crystal structure. *Can. Mineral.*, **27**, 427-440.
- Hussak, E. & Prior, G.T. (1897): On derbylite, a new antimono-titanate of iron from Tripuhy, Brazil. *Mineral. Mag.*, **11**, 176-179.
- Konev, A.A., Reznitsky, L.S., Feoktistov, G.D., Sapozhnikov, A.N., Koneva, A.A., Sklyarov, E.V., Vorobyev, E.I., Ivanov, V.G., Ushchapovskaya, Z.F. (2001): Mineralogy in the East Siberia: State of the art on the threshold of XXI Century. New and rare-occurring minerals (in Russian). ed. Konev, A.A., Intermet Engineering, Moscow, Russia, 240 p.
- Krzemnicki, M.S. & Reusser, E. (1998): Graeserite, Fe₄Ti₃AsO₁₃(OH), a new mineral species of the derbylite group from the Monte Leone nappe, Binntal region, Western Alps, Switzerland. *Can. Mineral.*, **36**, 1083-1088.
- Moore, P.B. & Araki, T. (1976): Derbylite, Fe³⁺Ti⁴⁺Sb³⁺O₁₃(OH), a novel close-packed oxide structure. *N. Jahrb. Mineral., Abh.*, **126**, 292-303.
- Nickel, E.H. & Grey, I.E. (1979): Tomichite, a new oxide mineral from Western Australia. *Mineral. Mag.*, **43**, 469-471.
- Reznitsky, L.Z. & Sklyarov, E.V. (1996): Unique Cr-V mineral association in metacarbonate rocks of the Sludyanka, Russia. 30th International Geological Congress, Beijing, China, p. 446.
- Reznitsky, L.Z., Sklyarov, E.V., Armbruster, T., Galuskin, E.V., Ushchapovskaya, Z.F., Polekhovskiy, Yu.S., Karmanov, N.S., Kashaev, A.A., Barash, I.G. (2007): Batisivite V₈Ti₆[Ba(Si₂O)]O₂₈ – A new mineral species of the derbylite group (in Russian). *Proc. Russ. Mineral. Soc.*, **136(5)**, 65-75.
- Shannon, R.D. (1976): Revised ionic radii and systematic studies of interatomic distances in halides and chalcogenides. *Acta Cryst.*, **A32**, 751-767.
- Schindler, M., Hawthorne, F.C., Baur, W.H. (2000): Crystal chemical aspects of vanadium: polyhedral geometries, characteristic bond valences, and polymerization of (VO_n) polyhedra. *Chem. Mater.*, **12**, 1248-1259.
- Strunz, H. & Nickel, E.H. (2001): Strunz Mineralogical Tables. Chemical-Structural Mineral Classification System. 9th ed., Stuttgart, Schweizerbart, 870 p.

Received 17 October 2007

Modified version received 9 January 2008

Accepted 10 January 2008